Hindawi
Wireless Communications and Mobile Computing
Volume 2018, Article ID 7068601, 12 pages
https://doi.org/10.1155/2018/7068601

Research Article

Development and Validation of New Reverberation Chamber for Wireless Devices

Dong-Uk Sim,[1] **Sang Il Kwak**,[1] **Jong Hwa Kwon**,[1] **and Seong-Ook Park**[2]

[1]*Radio Environment and Monitoring Research Group, Electronics and Telecommunications Research Institute (ETRI), Daejeon 34129, Republic of Korea*
[2]*School of Electrical Engineering, Korea Advanced Institute of Science and Technology (KAIST), Daejeon 34141, Republic of Korea*

Correspondence should be addressed to Dong-Uk Sim; simdonguk@etri.re.kr

Received 19 April 2018; Accepted 23 May 2018; Published 26 June 2018

Academic Editor: Haejoon Jung

This paper proposes a reverberation chamber structure consisting of new reflectors and mode stirrers for electromagnetic compatibility and wireless terminal measurements. The key design considerations for them are determined through a reasonable approach to analyze the eigenmode for a reverberation chamber and the standard deviation of its working volume based on 3D simulation. The final designs are expected to improve the standard deviation performance of the initial structure of the reverberation chamber and provide a better mode stirring environment. The results measured in the fabricated chamber demonstrate that these predictions are clearly realized. The results satisfy the main requirements of this paper, which are defined in consideration of the specifications of commercial reverberation chamber products. Therefore, the reverberation chamber of this paper is expected to be useful for performance measurement and evaluation of commercial wireless terminals. To verify this logical approach to obtain a good design and its results, the results measured in the actual fabricated reverberation chamber are described along with analytical and computational results.

1. Introduction

Unlike previous generations, 5G network is characterized by the provision of innovative services rather than technological advances [1]. ITU-R proposed the service scenarios for 5G such as augmented reality (AR), self-driving car, and smart city cameras, which are defined as a combination of the following three core scenarios: enhanced mobile broadband (eMBB), ultra-high reliable and low latency communications (URLLC), and massive machine type communication (mMTC) [2]. The innovative services impose very challenging requirements on 5G network, such as the 1000 times higher data rate and 100 times reduced latency, which are impossible to meet with a single technology. Therefore, a wide variety of devices equipped with suitable technologies for each service will comprise the 5G network. For the wide variety of devices, providing a single measurement instrument such as an anechoic chamber (AC) or a reverberation chamber (RC) is one of the important issues to reduce capital and operational expenses (CAPEX/OPEX).

The AC has been considered the only way to measure the 5G devices. However, to overcome drawbacks of AC as well as considering the real communication environment, recently the RC attracts a huge attention. The RC is an important alternative measurement instrument for the measurement and application of small antennas for wireless and mobile terminals and for realistic evaluation of SISO to MIMO devices below the current 4G standard, as is well known through the IEC 61000-4-21 standard [3–5]. It can be used for obtaining various metrics between traditional antennas and devices such as efficiency, correlation, total radiated power (TRP), and total isotropic sensitivity (TIS) with high accuracy and short measurement times. Currently, the widespread use of this RC technology provides a variety of methodologies to support testing of the key performance indicators for 5G devices. However, achieving this requires the design of RC that has a more stringent field uniformity performance than the standard, which is for electromagnetic compatibility (EMC), not for 5G services. This is because, at higher frequencies in the millimeter wave band that will be a key component

for enabling a massive increase of the available bandwidth and high data rates, the measurement uncertainty may have a profound effect on the actual performance evaluation of 5G devices. Thus, more stringent user requirements for an RC must be defined, and a reasonable design approach is required to achieve them.

The most important consideration for the intended measurement tasks and applications in these fields is to design an RC appropriately so that it satisfies the user's requirements. The standard provides requirements of acceptable RC performance and basic guidelines for RC design to meet these requirements. Indeed, there are no indicators to objectively evaluate RC performance beyond the requirements of the standard in modeling for RC construction. Also, even if an RC is designed much more stringently than the requirements proposed in the standard, this does not prove that it can achieve superior performance in comparison to other RCs. In other words, comparing the performance of different RCs, including their physical parameters, can be quite difficult, and there are no theoretically standardized formats or guidelines on how to carry out RC modeling to achieve better performance.

In this respect, it can be said that the design of an RC with excellent performance is virtually impossible without an initial reference structure. Based on an initial structure that satisfies the basic standard guidelines, the specific design of an RC should follow a reasonable structure design process to modify it until the user's own requirements are satisfied. The derivation of this initial structure and the logical process for its improvement are dependent on known rules of thumb or unknown rules of thumb [6, 7]. It is well known that a deterministic approach based on the numerical method is accurate in modeling an RC including mode stirrers for desired RC performance [8]. Based on this approach and the rules of thumb, the RC design method based on 3D electromagnetic wave (EM) simulations provides valuable insight into the physical working principles of an RC; allows the design behaviours for the geometrical parameters, such as mode stirrer size, shape, and position to be determined; and finally shortens the development time until the RC meets all the requirements of the user [9]. We can refer to other RC structures introduced in other papers for purposes different from this study, which include several types of mode stirrers [10–12].

This paper proposes a new RC structure for EMC and wireless device measurements. As mentioned above, the requirements for an RC have been established and its initial structure has been determined through the references and the rules of thumb. Based on the initial structure, a reasonable approach using field uniformity and eigenmode analysis in the RC has resulted in the final structure that satisfies the requirements and shows improved performance compared to the initial one. Another objective of this paper is to show that this approach for superior design will improve the previous results in a way that compares relatively well with the current theoretical results. To verify the performance of the final structure, experimental results of the constructed prototype are presented along with simulation results.

Table 1: Requirements of reverberation chamber to develop.

Items	Requirements
Start operating frequency	650 MHz
Overall volume	5.05 m^3
(Internal dimensions)	(1.4 m × 1.95 m × 1.85 m)
Working volume	0.76 m^3
(Rectangular dimensions)	(0.835 m × 0.951 m ×0.954 m)
Standard deviation	Less than 2.5 dB

2. Reverberation Chamber Requirements

Considering the requirements of the IEC 61000-4-21 standard, the requirements of RC to be developed in this work are shown in Table 1. For measurements at mobile communication frequencies and for EMC measurements above 1 GHz, the start operating frequency of the RC was set to 650 MHz [13, 14]. The RC has inner dimensions of 1.4 m × 1.95 m × 1.85 m (length L × width W × height H) based on the size of the Bluetest RTS60 model, having outside dimensions of 1.4 m × 1.94 m × 2 m [15].

The working volume of the RC can be located at a distance greater than $\lambda/4$ from the wall, mode stirrers, and reflectors within the RC [3], where λ is the wavelength for the start operating frequency of the RC. If the distance from them is selected as $\lambda/4$, the working volume will be the maximum size. If the requirement for field uniformity is met, the larger the working volume, the better the usability. However, in the process of designing an RC to meet the user's requirements after they are defined by the procedure introduced in this paper, there can be a risk that the mode stirrer or reflector structures satisfying the field uniformity condition may not be derived when the maximum working volume is defined. Moreover, there is also the drawback that it can take a long time to find the structures. Therefore, the working volume should be set appropriately considering the size of the device under test (DUT) as well as the position and distance from the mode stirrers and reflectors.

To do this, commercial RCs (whose overall size and the working volume dimensions are published) were investigated, and the ratio between them was analyzed. This is not based on theoretical grounds, but only to figure out the average level of the ratio from those designed cases. In the case of Siepel models, EOLE80, EOLE200, EOLE400, and EOLE1000 models, the ratios were approximately 10%, 17%, 19%, and 16%, respectively [16]. In this case, the field uniformity specification applied is 3 dB. Considering these data and the standard deviation requirement of this study, the ratio was set to approximately 15%, and the corresponding working volume dimensions were determined as 0.835 m × 0.951 m × 0.954 m (length W_L × width W_W × height W_H), as shown in Table 1. The general standard deviation, a field uniformity requirement of the IEC 61000-4-21 standard, is 3 dB, but in this study it was set to a more stringent value of 2.5 dB.

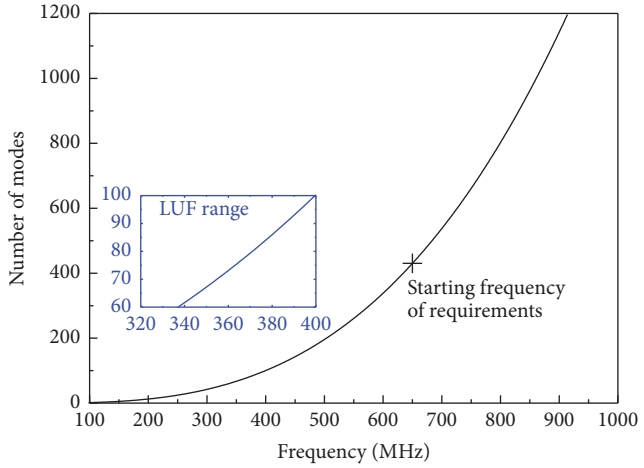

Figure 1: Theoretical number of modes for a reverberation chamber of the size considered in this paper.

The number of modes N computed approximately above cutoff in an ideal empty cavity is given by

$$N = \frac{8\pi}{3}(L \times W \times H)\frac{f^3}{c_0^3}, \quad (1)$$

where f is the frequency in hertz and c_0 is the vacuum speed of light in meters per second [17]. For the overall size of the RC in Table 1, the modal numbers present in the cavity with respect to the frequency are shown in Figure 1. The "60 to 100 modes" rule suggests that the lowest useable frequency (LUF) exists in the range of approximately 338 MHz to 400 MHz [3, 18]. For the purpose of this work, 650 MHz, at which many more modes are generated than at the theoretical LUF, is considered as the start operating frequency of RC, that is, the actual LUF. Therefore, the RC performance was considered starting from 650 MHz during the development process and verification.

3. Reverberation Chamber Design and Simulation

3.1. The Basic Prototype of Reverberation Chamber. The basic prototype of the RC that reflects the dimension requirements in Table 1 is shown in Figure 2. It is a rectangular chamber consisting of two mode stirrers, herein referred to as stirrer 1 and stirrer 2. Stirrer 1 is perpendicular to the bottom of the chamber and consists of four rectangular planes with a width (a) of 0.46 m and a height (b) of 0.46 m, which correspond to the size of one wavelength for an operating frequency of 650 MHz. For asymmetric placement between all planes, these planes have been rotated 45° around rotation axes with the directions of $(\vec{x} + \vec{y} + \vec{z})$, $(\vec{x} - \vec{y} + \vec{z})$, $(-\vec{x} - \vec{y} - \vec{z})$, and $(-\vec{x} + \vec{y} + \vec{z})$ at each of their centers in order from the plane nearest to the bottom.

Stirrer 2 is horizontal to the bottom of the chamber and consists of four rectangular planes. Taking into account operation at the higher frequency and the asymmetry of stirrer 1, each plane has a width (c) of 0.4 m and a height (d) of

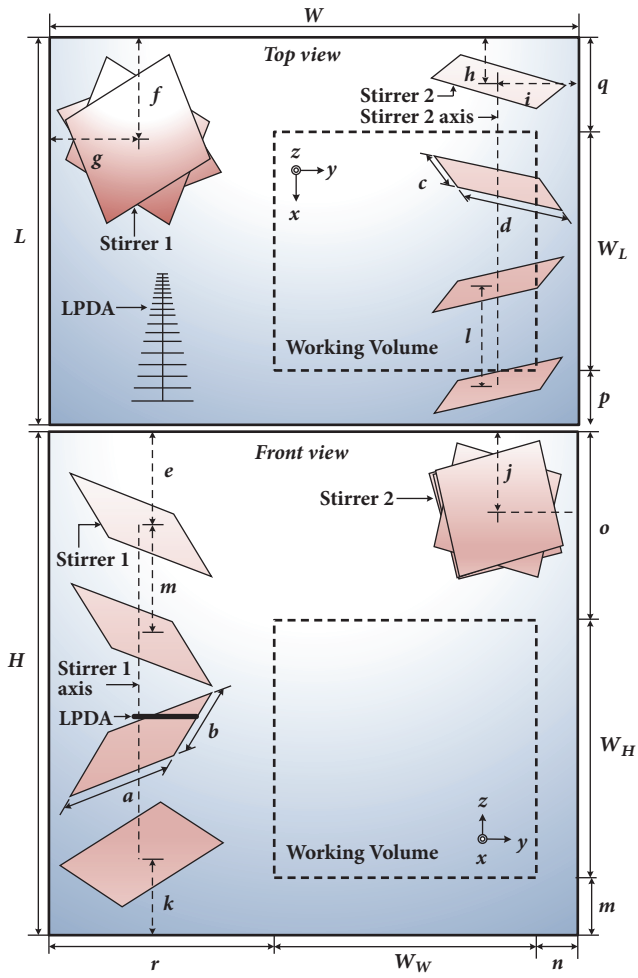

Figure 2: Basic prototype of a reverberation chamber proposed in this paper.

0.4 m, which are slightly less than one wavelength. Similarly, these planes have also been rotated 25° around rotation axes with the same vector directions as in the case of stirrer 1 at each of their centers in order from the bottom plane in the top view of Figure 2. The working volume defined in Table 1 is located 0.157 m from stirrer 1 and 0.12 m from stirrer 2. These are spaced distances greater than 0.115 m, which is a quarter wavelength for an operating frequency of 650 MHz [3]. Likewise, the separation distances from the RC walls, denoted by m, n, p, and q, were determined to be more than a quarter wavelength and satisfy the working volume requirement of Table 1. The values of all parameters depicted in Figure 2 are shown in Table 2.

To investigate the level of field uniformity of the basic prototype as described in Introduction, a commercial software package FEKO as the simulation kernel, which is based on a frequency domain method of moment (MOM), is used [19]. Because it provides ease of modeling large 3D structures, such as an RC, as well as its numerical accuracy, it was chosen for this study. The algorithms and the usability of the software can be confirmed through several published studies that have used them in analyzing RCs [8–10], although those studies

Table 2: Design parameters for the basic prototype of the reverberation chamber.

Parameter	Length, m	Parameter	Length, m
H	1.85	g	0.34
L	1.4	h	0.16
W	1.95	i	0.31
W_H	0.954	j	0.3
W_L	0.835	k	0.3
W_W	0.951	l	0.36
a	0.46	m	0.2
b	0.46	n	0.2
c	0.4	o	0.7
d	0.4	p	0.2
e	0.35	q	0.364
f	0.36	r	0.8

may have had purposes different from that of the present study.

For the simulation of the materials in the closed structure, a free space condition with a relative permittivity of $\varepsilon_r = 1$ and a relative magnetic permeability of $\mu_r = 1$, which were assumed to be frequency independent, was used. For the zinc plates of the RC walls and the aluminum plates of mode stirrers with a thickness of 0.002 m, the values of $\sigma = 1.67 \times 10^7$ S/m and $\sigma = 3.816 \times 10^7$ S/m, respectively, were used. These values were also assumed to be frequency independent. The processor and memory used for the simulations were an Intel(R) Xeon(R) CPU E5-2699 v4 and a memory (RAM) of 256 GB, respectively.

The simulations were performed at a total of nine frequencies at 25 MHz intervals from 650 MHz to 850 MHz. The reason is that for 850 MHz and above, the mesh size generated in the RC requires much more resources to compute. A log-periodic dipole array (LPDA) antenna was used as a transmitting antenna for the simulations. It consisted of 18 dipole elements, and it was realized by impedance matching through the transmission line network. At each calculation frequency, a total of twenty simulations were performed as the stirrers rotated at 18° intervals. Then, the standard deviation representing the field uniformity of the RC was computed according to the IEC 61000-4-21 standard after postprocessing collecting the electric field data from twenty simulations.

The results are shown in Figure 3. These results show that the basic prototype of the RC, which reflects the physical requirements in Table 1, exhibits a standard deviation characteristic of less than 3 dB at most frequencies. These simulations were not intended to calculate accurate standard deviation values, but rather to investigate the tendency of their change and their approximate level in the frequency band of interest. In actual measurements, it was expected that a lower standard deviation could be obtained because the reverberation effect occurs constantly, while the stirrers rotate at regular intervals. Based on the basic structure, the following subsections describe its performance improvement process and the corresponding results to meet the performance requirements of Table 1.

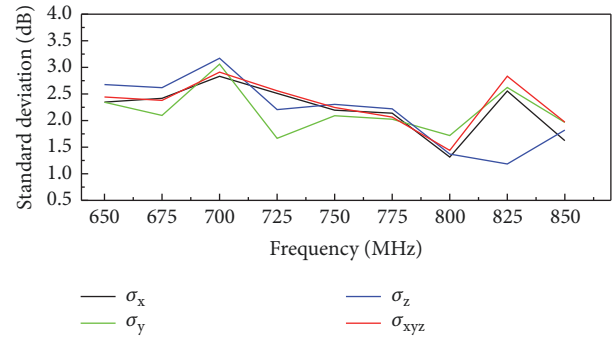

Figure 3: The simulated E-field standard deviation for working volume of the basic RC structure.

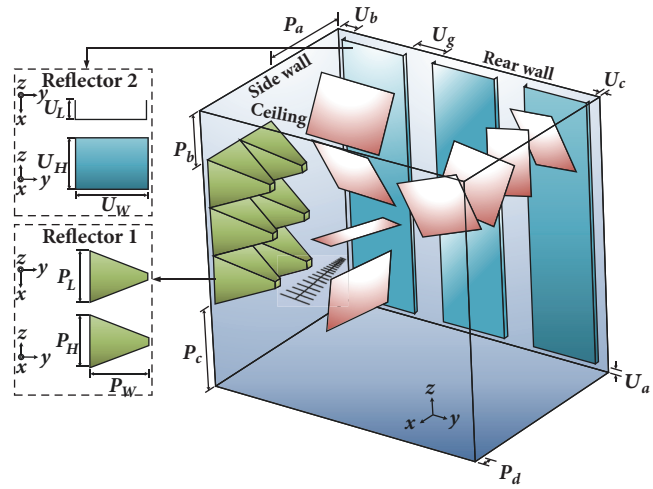

Figure 4: RC structure with reflector 1 and 2.

3.2. The Effect of Reflectors in a Reverberation Chamber. The approach to improve the field uniformity of an RC can be roughly divided into two main aspects. One of them is to implement the appropriate reflectors by effectively utilizing the empty spaces on the RC walls. The other is to design efficient mode stirrers. This part describes the results for the former. As shown in Figure 2, due to the mode stirrers and the working volume, the available wall space is limited to the space on the walls forming the edges under stirrer 1 in the top view and the ceiling space between stirrer 1 and stirrer 2 in the front view.

The reflector structures and their positions applied to these spaces are shown in Figure 4. The structure of reflector type 1 is derived from the shape of a pyramidal absorber in a typical anechoic chamber. Taking into account the space required to place multiple reflectors and space to place the transmitting antenna, reflector type 1 has dimensions of 0.324 m × 0.36 m × 0.324 m. In addition, their final positions were determined through a parametric study analyzing the field uniformity according to those numbers.

Figure 5 shows the variation of standard deviation according to the number of type 1 reflectors. These results were calculated by placing them in order from the bottom of the left sidewall to the top, in the top of the middle of the

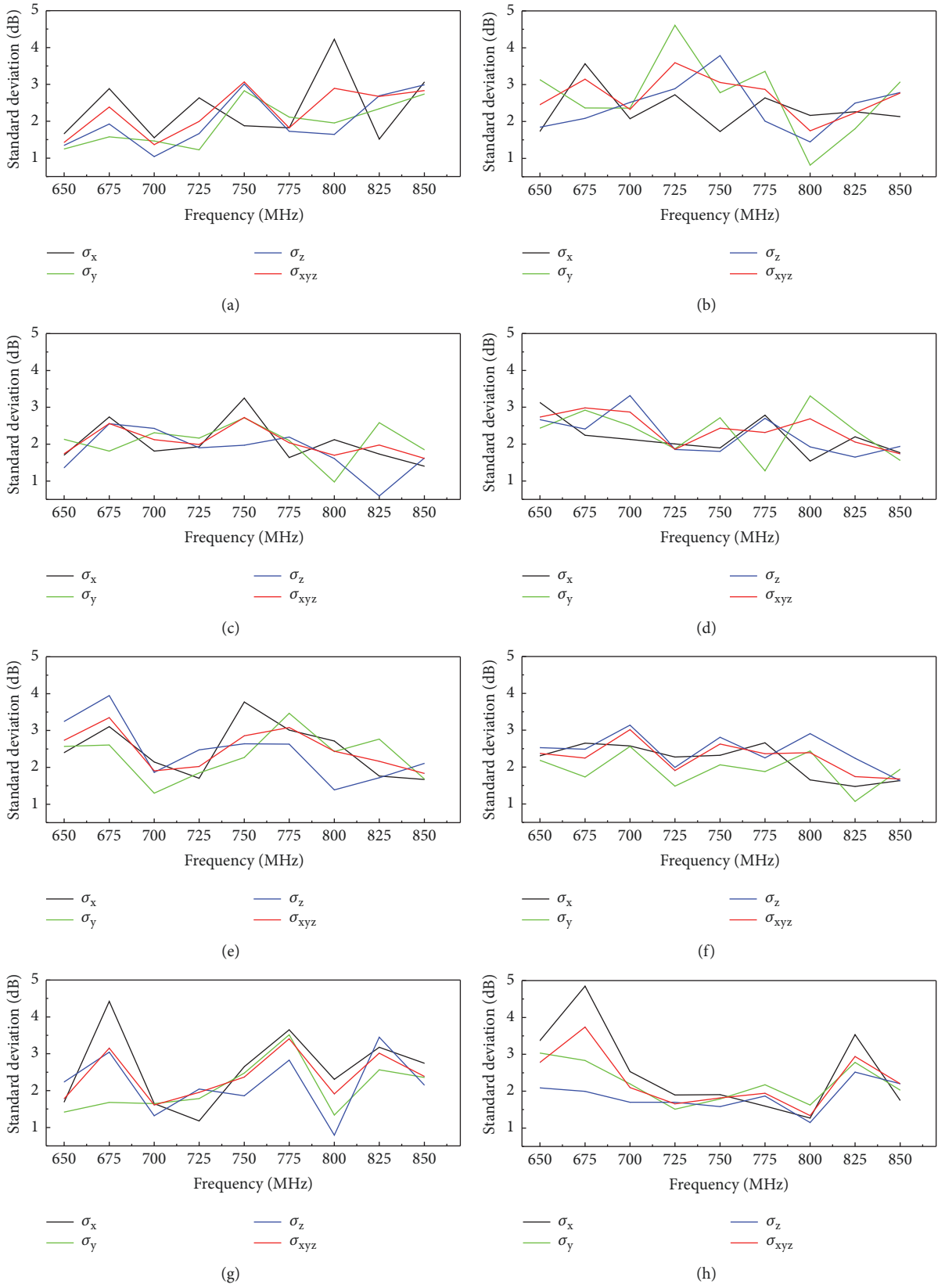

FIGURE 5: Standard deviation calculated according to the number of reflector 1 when there is no reflector 2. (a) 2. (b) 4. (c) 6. (d) 8. (e) 10. (f) 11. (g) 13. and(h) 16.

Table 3: Design parameters related to the reflectors within the reverberation chamber.

Parameter	Length, m	Parameter	Length, m
P_H	0.324	U_H	1.75
P_L	0.324	U_L	0.03
P_W	0.36	U_W	0.461
P_a	0.71	U_a	0.05
P_b	0.34	U_b	0.05
P_c	0.538	U_c	0.05
P_d	0.042	U_g	0.22

rear wall, and in the space between stirrers 1 and 2 on the ceiling in the absence of type 2 reflectors in Figure 4. For the simulations, various numbers of type 1 reflectors were located in the RC that is eight, two, and six, respectively, and a total of sixteen simulation results were obtained. The numbers in the upper right corner of the graphs in Figure 5 indicate the number of type 1 reflectors applied.

The results indicates that when six type 1 reflectors are located on the left wall as shown in Figure 5(c), an acceptable standard deviation is obtained in the frequency band of interest. Here, when the number of type 1 reflectors is fixed to six, the standard deviation is recalculated according to the numbers of reflectors placed on the rear wall and the ceiling. The results were found to be similar or worse than that obtained with six type 1 reflectors. Therefore, it can be said that the number of type 1 reflectors should be six in consideration of convenience and cost in the fabrication of an RC. The final design parameter values for reflector 1 are shown in Table 3.

Placing reflector 2 shown in Figure 4 on the rear wall of the RC makes part of the wall uneven; thus, we can expect the generation of hybrid modes that can contribute to making the field evenly distributed in the RC. This expectation is based on the acoustical theory that the acoustical quality of a room can be improved by using scattering elements [20]. However, the structure of reflector 2 proposed in this paper, which are different from the scattering elements, was chosen as a thin plate attached to the chamber wall with a thin air gap (U_L) between the plate and the wall.

As described above, the standard deviation analysis method of the working volume for evaluating field uniformity is very intuitive, but it does not provide a valuable insight into the physical principles caused by changes in structures, including mode stirrers inside an RC. In addition, the method requires extensive computation time, computational resources, and complex postprocessing. From this point of view, eigenmode analysis is very effective for the design of mode stirrers or reflectors in an RC. According to this technique, the design with the maximum amount of eigenfrequency shifts is the optimal choice, which allows designers to quickly and easily evaluate designs. This was confirmed in [21], which stated that the effectiveness of a mode stirrer lies in its ability to shift eigenfrequencies.

It should be noted that it is very difficult to quantitatively define the correlation between the eigenfrequency shift and the standard deviation of the field uniformity. Therefore, the eigenfrequency and standard deviation should be analyzed together based on the reference structure, for example, as shown in Figure 2, to obtain the field uniformity satisfying the user's requirements. The eigenfrequency shifts (Δf_{eigen}) are given by

$$\Delta f_{\text{eigen}} = \left| f_{\text{eigen.empty}} - f_{\text{eigen.loaded}} \right|, \tag{2}$$

where $f_{\text{eigen.empty}}$ and $f_{\text{eigen.loaded}}$ are the eigenfrequencies in an empty cavity and in an RC including each subsequent design in the cavity, respectively. According to (2), all designs presented in this section are evaluated under the same conditions, and the relative performance is compared. The eigenfrequencies are calculated for the actual total volume and internal structures of the RC shown in Figures 2 and 4 by using CST MICROWAVE STUDIO [22]. The material filling the RC is air (free space), and for a numerical analysis the boundary conditions selected on all its walls are $E = 0$.

Table 4: Dimensions for width and gap of type 2 reflectors for the eigenfrequency shifts analysis according to their number.

Number of Reflector 2	U_W, m	U_g, m	Other Parameters
4	0.24	0.24	Same as Table 3
5	0.24	0.12	
8	0.12	0.12	
9	0.12	0.06	
11	0.06	0.12	
12	0.12	0.03	
21	0.06	0.03	

For the calculation of eigenfrequencies according to the number of type 2 reflectors, their width (U_W) and spacing (U_g) were selected as shown in Table 4. Other parameters were the same as those shown in Tables 2 and 3. This is to investigate the changes in eigenfrequencies within an RC depending on the degree of roughness. The calculated results are shown in Figure 6. No consistent relevance for the changes in U_g can be found in three pairs of results obtained when the number of type 2 reflectors is 4 and 5, 8 and 9, and 11 and 21. Likewise, the three pairs of results when the number of type 2 reflectors are 5 and 8, 8 and 11, and 12 and 21 do not show any linear relationship for the variation of U_W. However, it can be seen that the amount of eigenfrequency shifts is larger under conditions where the number of type 2 reflectors is small and their width is large. In particular, it should be noted that the width corresponds to approximately $\lambda/4$ of the starting operating frequency. From these results, the eigenfrequencies were investigated for several dimensions of U_W and U_g when a smaller number of type 2 reflectors were applied, that is, when 2 or 3 reflectors were applied. Those conditions are shown in Table 5.

The numerical results shown in Figures 6(b) and 6(c) show that the conditions of $U_W = 0.461$ m and $U_g = 0.22$ m can provide a better environment than other conditions in terms of the mode stirring performance of the RC. In particular, this condition in which the width corresponds to approximately

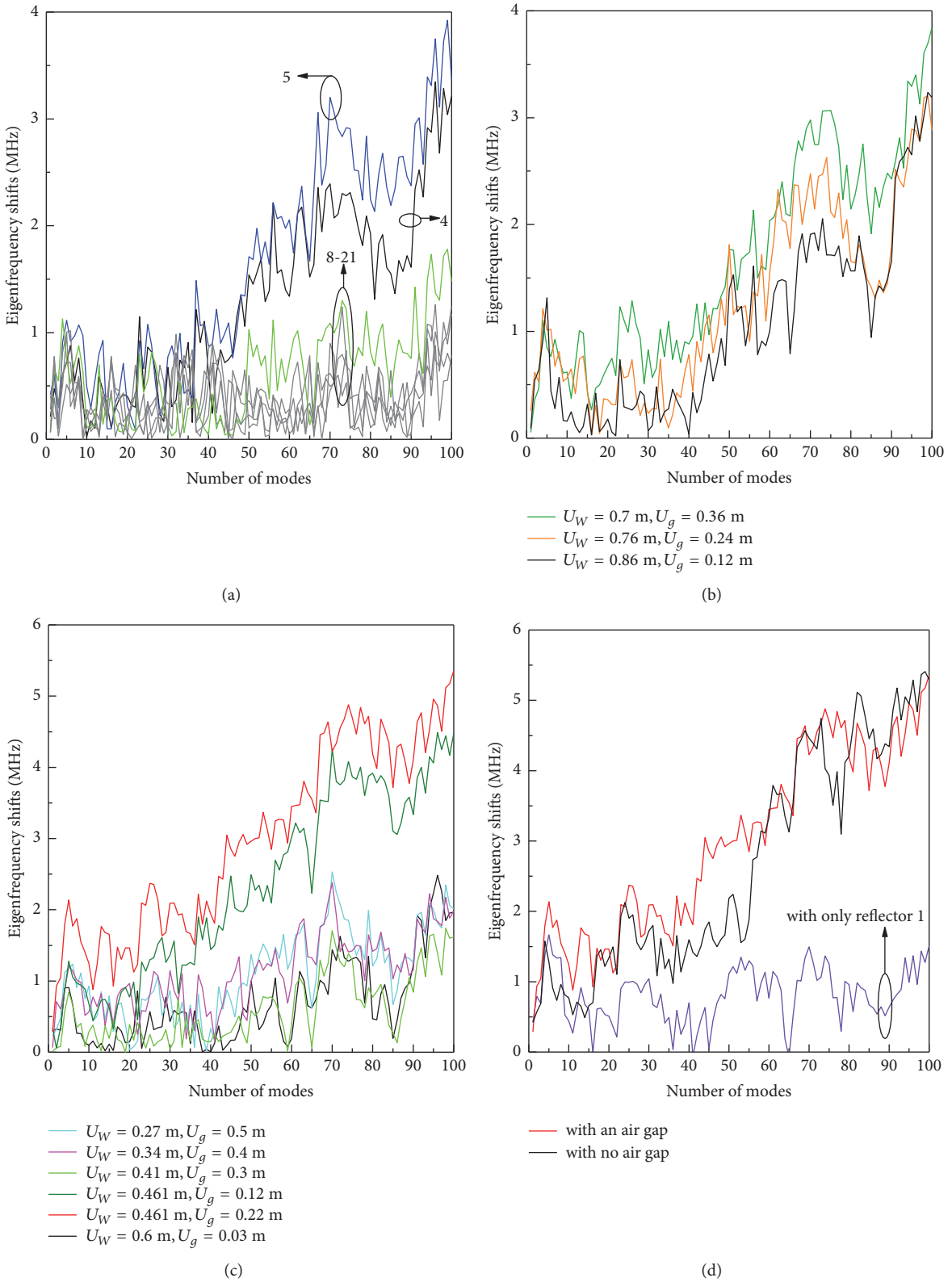

FIGURE 6: Eigenfrequency shifts calculated to determine the dimensions of reflector 2. (a) Results for the conditions in Table 4. (b) Results for two reflectors of the conditions in Table 5. (c) Results for three reflectors in Table 5. (d) Comparison of results for type 2 reflectors with an air gap and with no air gap when $U_W = 0.461$ m and $U_g = 0.22$ m.

Table 5: Dimensions for width and gap of type 2 reflectors for the eigenfrequency shifts calculations.

Number of Reflector 2	U_W, m	U_g, m	Other Parameters
2	0.7	0.36	Same as Table 3
	0.76	0.24	
	0.86	0.12	
3	0.27	0.5	Same as Table 3
	0.34	0.4	
	0.41	0.3	
	0.461	0.12	
	0.461	0.22	

one wavelength (λ) shows an improved performance over $\lambda/2$ and $3\lambda/2$ conditions of $U_W = 0.24$ m and $U_W = 0.7$ m in Figure 6(a), respectively. Figure 6(d) shows that type 2 reflectors with an air gap shown in Figure 4 are superior to type 2 reflectors with no air gap in most modal numbers as well as lower ones and provides evidence that the shape of reflector 2 with the dimensions described above can create a better mode stirring environment than when there is only reflector 1.

3.3. Mode Stirrer Design and the Final Design Results of RC. In the RC shown in Figures 2 and 4, it can be inferred that there is a limit to the mode stirrer design to improve the mode stirring performance. First, the method of constructing the additional mode stirrer is difficult to realize spatially because of the working volume already defined and the transmitting antenna. Moreover, it is not efficient in terms of production cost because a separate motor for rotating the mode stirrer must be introduced. An alternative is to directly modify the structures of stirrers 1 and 2. This may have the effect of increasing the electrical length of the stirrer plates by making each square plate of the stirrers asymmetrically irregular. However, the start operating frequency of the RC defined in this paper is 650 MHz, which is much larger than the theoretical LUF, as described in Section 2, and performance improvements at frequencies lower than that are beyond the scope of interest. Even if there is room for improvement beyond the start operating frequency, the ease and cost of fabrication should be considered in reality for more complex structures. It should also be noted that the field uniformity performance at around 650 MHz in the results of number 6 of Figure 5 shows a level that almost satisfies the requirements. Therefore, a relatively simple approach has been adopted in this paper.

Figure 7 shows the final RC structure with the new stirrers 1 and 2 consisting of dual plates. In the case of stirrer 1, the newly added plates are located at the top of each pair. Also, in the case of stirrer 2, the new plates are located closer to the front, including the door, in each pair. The added plates have the same size as the original plates, and they are located at regular intervals denoted by g_{s1} and g_{s2} in the direction perpendicular to the plane from the center of the original ones. The performance of eigenfrequency shifts according

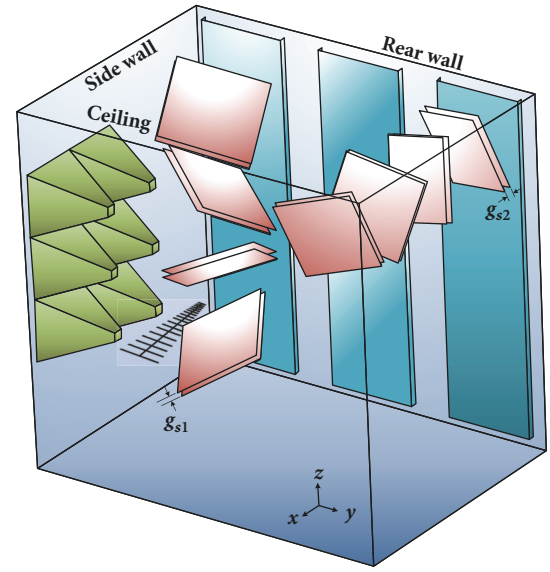

Figure 7: Final reverberation chamber structure with dual-plate type mode stirrers for fabrication.

to the intervals, g_{s1} and g_{s2}, is investigated as shown in Figure 8. Both graphs consistently show that the smaller the spacing of the plates that make up each stirrer, g_{s1} and g_{s2}, the better the eigenfrequency shifts occur. In addition, it has been confirmed again that the condition of $g_{s1} = g_{s2} = 0.03$ m, which is the minimum dimension for easy fabrication, must be chosen through calculation of the total 16 conditions for the dimensions of the parameters shown in the legend of both graphs.

The eigenfrequency shifts for the final design shown in Figure 7 are shown in Figure 9, along with the results from the previous step. The clear effect of the new stirrers can be seen after the tenth mode number. Also, it can be confirmed that the RC consisting of reflectors and new stirrers can provide a better environment in terms of mode stirring performance. In the proposed RC design, many parameters have not been analyzed. It is almost impossible to find the optimal condition by analyzing the correlations between all these variables, and doing so would have little advantage from the engineering viewpoint. Therefore, in this paper, a basic prototype RC has been derived based on rules of thumb, and methods for improving its performance have been proposed. In addition, by analyzing the key parameters corresponding to the methods through a reasonable approach, the final design that allows the performance of the manufactured RC to meet the requirements has been proposed.

The standard deviations calculated through 3D simulations and postprocessing to confirm the field uniformity performance of the final design are shown in Figure 10 along with the results for the other two conditions shown in Figure 9. The standard deviation results ultimately demonstrate the possibility of improving the mode stirring environment implied by the eigenfrequency shifts shown in Figure 9. In Figure 10(b), the results obtained with the addition of reflector 2 show a standard deviation of less than 3 dB at all analysis

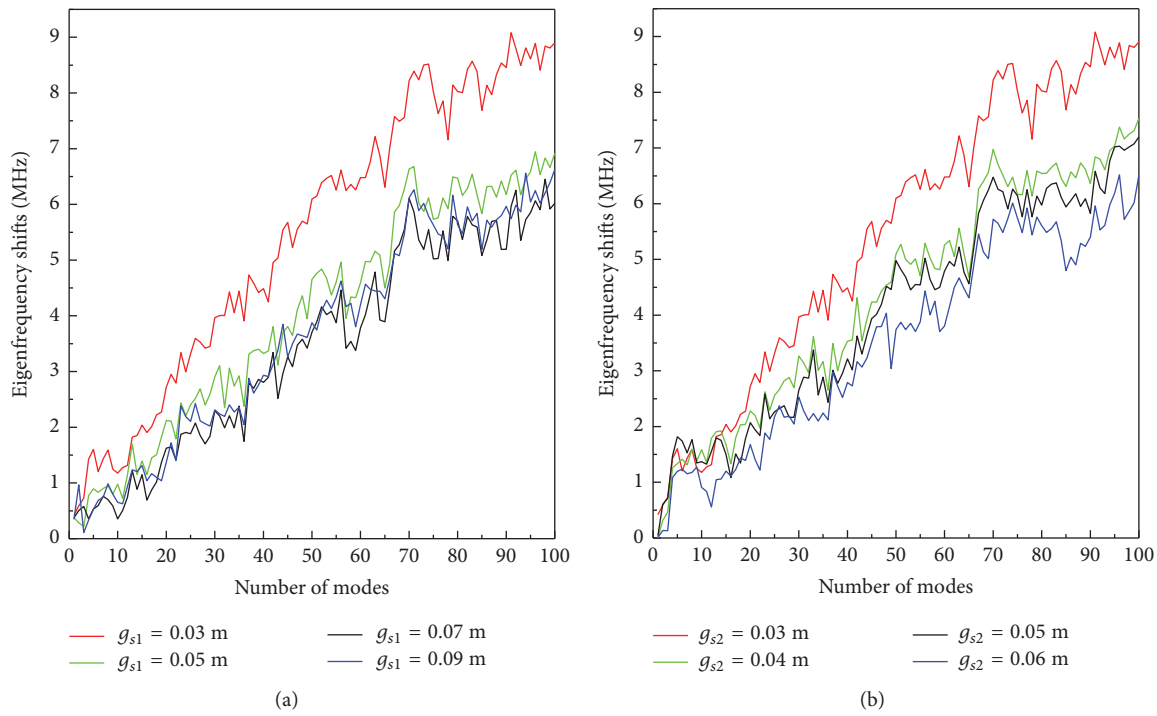

Figure 8: Calculated eigenfrequency shifts for RC with stirrers 1 and 2 in dual-plate form (a) when g_{s2} = 0.03 m and (b) when g_{s1} = 0.03 m.

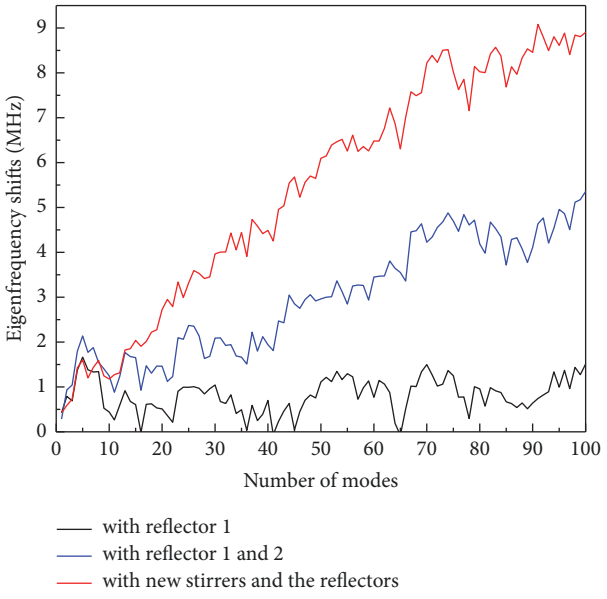

Figure 9: Eigenfrequency shifts for the final design compared to those of two other conditions shown in Figure 6(d).

frequencies compared to those in Figure 10(a). The results shown in Figure 10(c), which were obtained from the final design, show that the level of the overall standard deviation is lower in the band above 725 MHz compared to results shown in (c), and the difference between the components at each frequency is reduced. They also show slightly larger standard deviations than 2.5 dB at some frequencies and a maximum standard deviation of about 2.72 at 725 MHz. However, actual measurements in reverberating environments in which mode stirrers rotate at regular intervals are expected to produce values lower than standard deviations calculated through simulations in which each rotational step is ideally uncorrelated and show a standard deviation of less than 2.5 dB which meets the requirements of this paper.

4. Reverberation Chamber Measurements and Practical Verification

The final design shown in Figure 7 was made according to the dimensions of Tables 2 and 3 and the new stirrers. Figure 11 shows photographs of the fabricated RC, depicting reflector 1, reflector 2, the new stirrers, and the source antenna orientated in the x direction. Each mode stirrer is rotated by stepper motors controlled by computer software. The LPDA antenna for use as a transmitting antenna is located by a support in the position shown in Figures 2 and 11. The LPDA antenna must operate at 650 MHz or higher and be compact because the space in which it is placed is narrow. However, since the LPDA antenna satisfying these characteristics was not commercially available, one was developed independently. Figure 12 shows a photograph of the developed LPDA antenna. Detailed results for this LPDA antenna are described in [23]. A Rogers RO4003 substrate was used to fabricate the LPDA antenna, and its overall size was 282 mm × 194 mm × 0.508 mm ($L \times W \times H$). The fabricated LPDA antenna was measured with a radome as shown in Figure 11. Thus, a compact LPDA antenna has been demonstrated to operate from 0.55 to 9 GHz and to

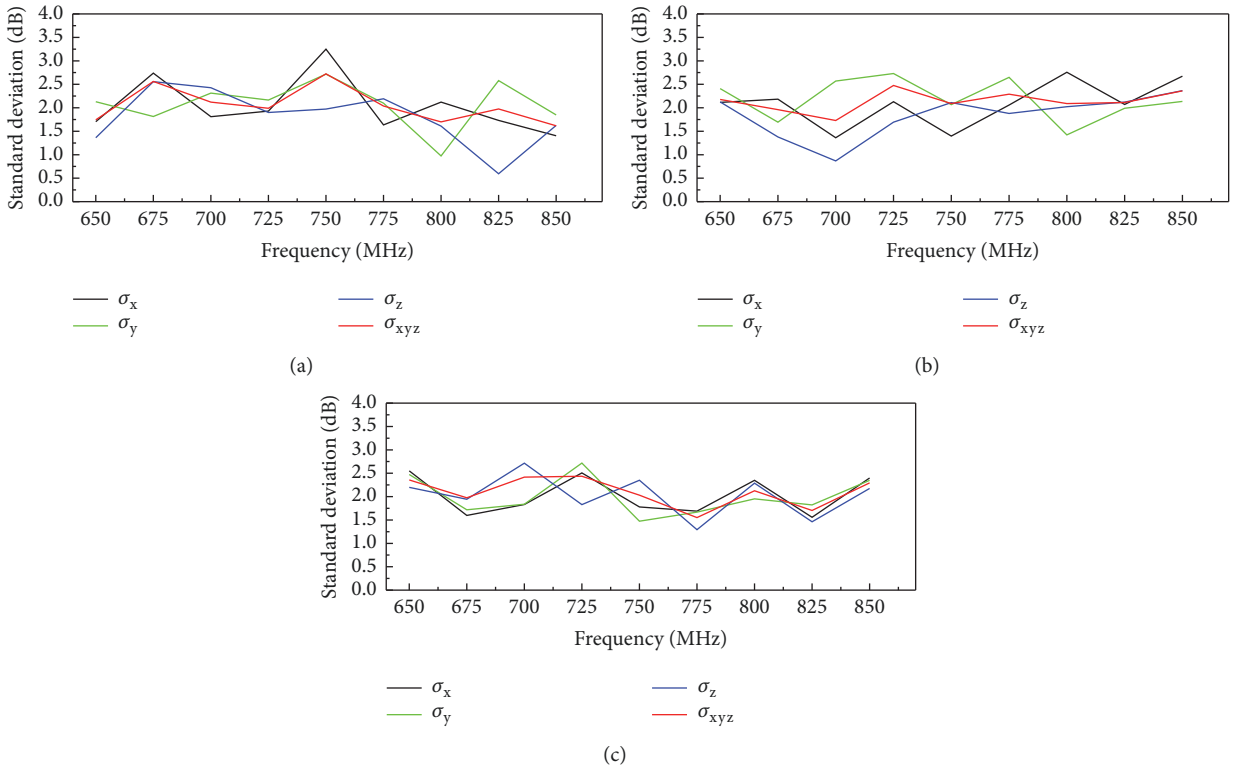

Figure 10: Calculated standard deviations for the RC (a) with reflector 1, (b) with reflectors 1 and 2, and (c) with the new stirrers and the reflectors, the final design.

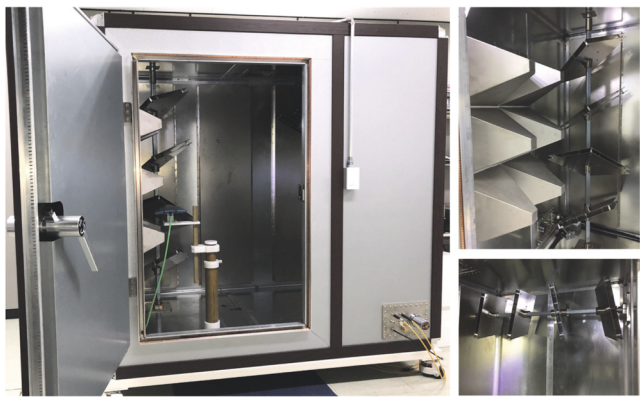

Figure 11: Photographs of the fabricated reverberation chamber.

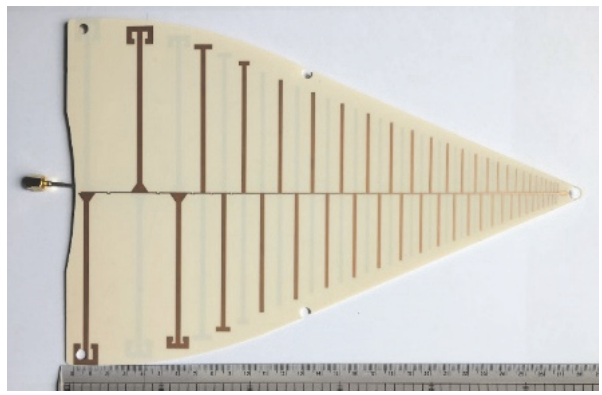

Figure 12: Photograph of the LPDA antenna developed to evaluate the performance of the proposed RC.

have a high gain ranging from 2.48 to 7.89 dBi. Compared to the standard LPDA antenna, the size of the proposed antenna has decreased by approximately 27% and 20% in length and width, respectively. Nevertheless, the miniaturized LPDA antenna exhibited broadband characteristics due to top loading techniques.

To evaluate the field uniformity performance of the proposed RC, the maximum electric field values were measured at eight corners of the working volume shown in Figure 2 based on the standard. An electric probe was used to record the field strengths, while the stirrer rotated through 18° angle steps (i.e., 20 positions for one turn of the stirrer). The standard deviation at each sample frequency was calculated from the raw data of the measured electric field. All measurements and calculations were in accordance with the guidelines proposed in [3].

Figure 13 details the standard deviations measured at the sampling frequencies specified by [3] for the proposed RC and shows its simulated standard deviations according to the design described in Section 3. The tolerance level of field uniformity defined in this paper, which is 2.5 dB, is also shown in the figure. The standard deviations in Figure 13(b)

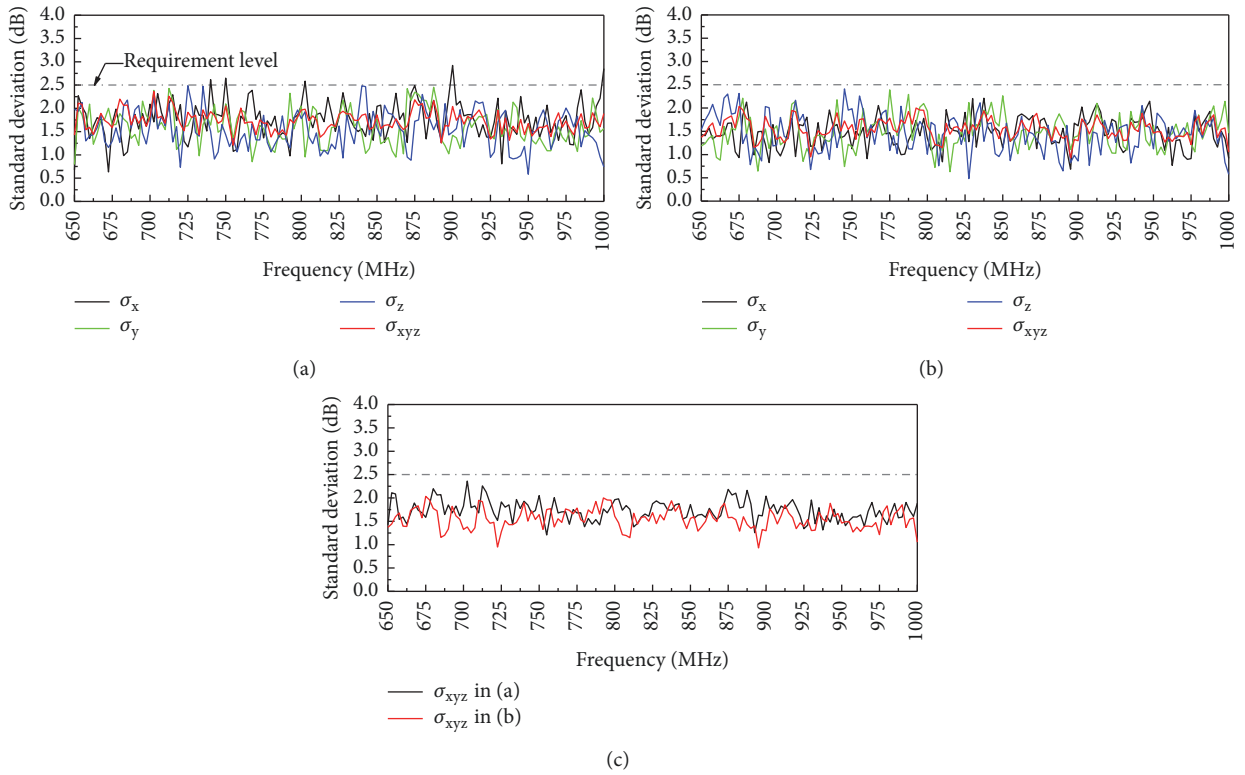

FIGURE 13: Measured standard deviations for the RC (a) with the reflectors and the original stirrers and (b) with the reflectors and the new stirrers, the final design. (c) Comparison between σ_{xyz} components of (a) and (b).

show that the final design consisting of the reflectors and the new dual-plate type stirrers meets the requirements for the field uniformity defined in this paper. It can also be seen that they are lowered at most frequencies compared to the results in Figure 13(a) obtained from a design composed of the reflectors and the original stirrers. This demonstrates that the new stirrer design outperforms the original design. In particular, remarkable frequency bands range from 680 MHz to 752.5 MHz and from 800 MHz to 935 MHz. The standard deviations are reduced by around 0.34 dB and 0.22 dB on average, respectively, and they are improved by up to 1 dB and 0.74 dB, respectively. In addition, the performance of the two stirrers is comparable at some frequencies. Based on these results, it can be concluded that the effective approach of this paper and the proposed final RC design shown in Figure 7 show a standard deviation below 2.5 dB by improving the performance of the basic prototype structure and satisfying all the defined requirements.

5. Conclusions

An RC consisting of new reflectors and mode stirrers has been proposed. It has an inner size that is approximately the same as or smaller than that of a commercial product. The main parameters for the reflectors and mode stirrers were determined through a logical approach based on standard deviation and eigenfrequency shift analysis by 3D simulations. The calculated and measured standard deviations for field uniformity evaluation of the proposed RC have demonstrated that they clearly improve the standard deviation performance of its initial structure. In addition, the reasonable approach proposed in this paper for the RC design is very effective, and it has been verified that the design results accurately predict the main results obtained from the actual measurements. The measured results for the standard deviation of the proposed RC were found to satisfy all of the requirements defined in this paper. Therefore, it is expected that the performance of the proposed RC could be a very attractive facility for users who want to measure and evaluate the performance of commercial wireless terminals.

Data Availability

The data used to support the findings of this study are available from the corresponding author upon request.

Conflicts of Interest

The authors declare that they have no conflicts of interest.

Acknowledgments

This work was supported by Institute for Information & Communications Technology Promotion grant funded by the Korea government (no. 2015-0-00855, Study on Measurement and Evaluation Technology based on Reverberation

Chamber, and no. 2017-0-00982, Development of System-Level Technology for Protection Design and Performance Evaluation against EMP). The authors are grateful to the staff of Korea Shield System Co., Ltd., the homepage of which is www.kshieldsysltd.com, for their help concerning the measurements in the reverberation chamber in this study.

References

[1] RWS-150029, "5G Vision and Enabling Technologies: ETRI Perspective," ETRI, 3GPP RAN workshop on 5G, Phoenix, AX, USA, 17^{th}-18^{th}, Sep. 2015.

[2] ITU-R WP5D, "Technical Performance Requirements (New Recommendation ITU-R Key Performance Indicator)," June 2017.

[3] "Reverberation Chamber Test Methods," International Electrotechnical Commission Standard IEC 61000-4-21: 2011, Jan. 2011.

[4] P.-S. Kildal, C. Carlsson, and J. Yang, "Measurement of free-space impedances of small antennas in reverberation chambers," *Microwave and Optical Technology Letters*, vol. 32, no. 2, pp. 112–115, 2002.

[5] P.-S. Kildal and K. Rosengren, "Correlation and capacity of MIMO systems and mutual coupling, radiation efficiency, and diversity gain of their antennas: simulations and measurements in a reverberation chamber," *IEEE Communications Magazine*, vol. 42, no. 12, pp. 104–112, 2004.

[6] A. Coates and A. P. Duffy, "Maximum working volume and minimum working frequency tradeoff in a reverberation chamber," *IEEE Transactions on Electromagnetic Compatibility*, vol. 49, no. 3, pp. 719–722, 2007.

[7] C. L. Zekios, P. C. Allilomes, M. T. Chryssomallis, and G. A. Kyriacou, "Finite element based eigenanalysis for the study of electrically large lossy cavities and reverberation chambers," *Progress in Electromagnetics Research B*, vol. 61, no. 1, pp. 269–296, 2015.

[8] H. Zhao and Z. Shen, "Memory-efficient modeling of reverberation chambers using hybrid recursive update discrete singular convolution-method of moments," *IEEE Transactions on Antennas and Propagation*, vol. 60, no. 6, pp. 2781–2789, 2012.

[9] C. Bruns and R. Vahldieck, "A closer look at reverberation chambers—3-D simulation and experimental verification," *IEEE Transactions on Electromagnetic Compatibility*, vol. 47, no. 3, pp. 612–626, 2005.

[10] G. Andrieu, F. Tristant, and A. Reineix, "Investigations about the use of aeronautical metallic halls containing apertures as mode-stirred reverberation chambers," *IEEE Transactions on Electromagnetic Compatibility*, vol. 55, no. 1, pp. 13–20, 2013.

[11] J. Clegg, A. C. Marvin, J. F. Dawson, and S. J. Porter, "Optimization of stirrer designs in a reverberation chamber," *IEEE Transactions on Electromagnetic Compatibility*, vol. 47, no. 4, pp. 824–832, 2005.

[12] A. Sorrentino, A. Gifuni, G. Ferrara, and M. Migliaccio, "Mode-stirred reverberating chamber autocorrelation function: Model, multifrequency measurements and applications," *IET Science, Measurement & Technology*, vol. 9, no. 5, pp. 547–554, 2015.

[13] "Electromagnetic compatibility of multimedia equipment-Emission requirements," International Electrotechnical Commission Standard CISPR 32: 2015, March 2015.

[14] "Electromagnetic compatibility of multimedia equipment-Immunity requirements," International Electrotechnical Commission Standard CISPR 35: 2016, August 2016.

[15] Reverberation chambers for MIMO OTA testing — BLUETEST.se, "Bluetest.se," 2018, https://bluetest.se.

[16] Accueil EN - siepel-www, "siepel-www," 2018, https://www.siepel.com.

[17] D. A. Hill, *Electromagnetic Field in Cavities: Deterministic and Statistical Theories*, John Wiley & Sons, Inc, New York, NY, USA, 2009.

[18] M. L. Crawford and G. H. Koepke, "Design, evaluation, and use of a reverberation chamber for performing electromagnetic susceptibility/vulnerability measurements," National Bureau of Standards NBS TN 1092, 1986.

[19] FEKO simulation software, "Overview of FEKO," http://www.feko.info.

[20] M. Mehta and J. Johnson, *Architectural Acoustics Principles and Design*, Prentice Hall, 1999.

[21] D. I. Wu and D. C. Chang, "The effect of an electrically large stirrer in a mode-stirred chamber," *IEEE Transactions on Electromagnetic Compatibility*, vol. 31, no. 2, pp. 164–169, 1989.

[22] CST MICROWAVE STUDIO software, "Overview of CST MICROWAVE STUDIO," http://www.cst.com.

[23] A. Kyei, D.-U. Sim, and Y.-B. Jung, "Compact log-periodic dipole array antenna with bandwidth-enhancement techniques for the low frequency band," *IET Microwaves, Antennas & Propagation*, vol. 11, no. 5, pp. 711–717, 2017.